Vibrational Properties of the One-Dimensional, $S = {}^1/_2$, Heisenberg Antiferromagnet Copper Pyrazine Dinitrate

B. R. Jones,*,† P. A. Varughese,† I. Olejniczak,†,|| J. M. Pigos,† J. L. Musfeldt,†,⊥ C. P. Landee,‡ M. M. Turnbull,‡ and G. L. Carr§

Department of Chemistry, State University of New York at Binghamton, Binghamton, New York 13902-6016, Department of Physics and Carlson School of Chemistry, Clark University, Worcester, Massachusetts 01610-1477, and National Synchrotron Light Source, Brookhaven National Laboratory, Upton, New York 11973-5000

Received December 21, 2000. Revised Manuscript Received March 12, 2001

We report the temperature-dependent infrared spectra of pure, deuterated, Zn-doped, and 2,6-dimethyl-substituted samples of the $S = {}^1/_2$, one-dimensional Quantum Heisenberg Antiferromagnet (QHAF) copper pyrazine dinitrate ($Cu(C_4H_4N_2)(NO_3)_2$). Of the more than 100 vibrational modes observed in the spectra, nearly one-third of them unexpectedly soften throughout the temperature range of investigation (300−5 K). We discuss the temperature dependence of the vibrational spectra in terms of several different models for mode softening. On the basis of detailed structural information and a comparison of the infrared spectra between pure copper pyrazine dinitrate and its chemically modified relatives, we conclude that the unusual softening observed in this low-dimensional molecular magnet is due to enhanced interchain hydrogen bonding with decreasing temperature.

I. Introduction

The concept of magneto-structural correlations by lattice engineering has been of great interest for decades.[1] If the magnetic properties of a material can be altered via chemical or structural modifications, the goal of ever better control over the design and resulting properties of molecular magnets can be achieved. For instance, it is possible to control the dimensionality of a magnetic solid through chemical modifications to the structure; $(C_nH_{2n+1}NH_3)_2MCl_4$, where M is a 3d metal ion, is an example.[2] Many compounds with a propensity for chemical tunability of magnetic properties, including $KMnO_4PO_4{\cdot}H_2O$,[3] $Ca_{2+x}Y_{2-x}Cu_5O_{10}$,[4] $Ni(C_2H_8N_2)_2NO_2ClO_4$ (NENP), and $Ni(C_2H_8N_2)_2NO_2PF_6$ (NENF),[5] have been investigated. Recent studies on Mn_{12}−acetate and related systems[6,7] reveal important quantum effects and add to the importance of lattice engineering in molecular magnets.

Our understanding of low-dimensional magnetic systems has been furthered by the investigation of magneto-structural correlations in bridged linear chain antiferromagnets. Copper pyrazine dinitrate, denoted CuPzN, is one such material, and is well represented by the $S = {}^1/_2$ QHAF model. $Cu(C_4H_4N_2)(NO_3)_2$ is highly one-dimensional; there is no indication of a transition to three-dimensional order down to 0.1 K, which implies that the ratio of interchain to intrachain coupling, $(J'/J) < 10^{-4}$.[8−10] The crystal structure is shown in Figure 1. It consists of linear chains of copper atoms in the crystallographic *a* direction, with each copper surrounded by two pyrazine molecules and two semichelating nitrate ions in a distorted octahedral arrangement. The pyrazine molecules lie at a 51° angle from normal to the basal plane, which is made up of the plane of the copper atom, the pyrazine nitrogen atoms, and the close oxygen atoms of the nitrate group. The path of the superexchange has been determined by neutron diffraction experiments to be through the pyrazine molecules.[9] The molecular structure of CuPzN provides many opportunities for the engineering of its lattice and subsequent magnetic interactions, which account for the popularity of this system.[11−18] These modifications include the possibility of substituting methyl groups on

* To whom correspondence should be addressed.
† State University of New York at Binghamton.
‡ Clark University.
§ Brookhaven National Laboratory.
|| Current address: Institute of Molecular Physics, Polish Academy of Sciences, Smoluchowskiego 17, 60-179 Poznan, Poland.
⊥ Current address: Department of Chemistry, University of Tennessee, Knoxville, TN 37976.

(1) *Magneto-Structural Correlations in Exchange Coupled Systems*; Willet, R. D., Gatteschi, D., Kahn, O., Eds.; Reidel Publishing, D.: Boston, 1983.

(2) Here, the interaction between magnetic monolayers can be made quite small by increasing the length of the alkyl chain ($n = 0$−15 or higher), effectively tuning between a three-dimensional and two-dimensional molecular magnet.[1]

(3) Fanucci, G. E.; Krzystek, J.; Weisel, M. W.; Brunel, L. C.; Talham, D. R. *J. Am. Chem. Soc.* **1998**, *120*, 5469−5479.

(4) Fong, H. F.; Keimer, B.; Lynn, J. W.; Hayashi, A.; Cava, R. J. *Phys. Rev. B* **1999**, *59*, 6873−6876.

(5) Landee, C. P.; Reza, K. A.; Bond, M. R.; Willet, R. D. *Phys. Rev. B* **1997**, *56*, 147−153.

(6) Friedman, J. R.; Sarachik, M. P.; Tejada, J.; Maciejewski, J.; Ziolo, R. *J. Appl. Phys.* **1996**, *79*, 6031−6033.

(7) Friedman, J. R.; Sarachik, M. P.; Hernandez, J. M.; Zhang, X. X.; Tejada, J.; Molins, E.; Ziolo, R. *J. Appl. Phys.* **1997**, *81*, 3978−3980.

(8) Villa, J. F.; Hatfield, W. E. *J. Am. Chem. Soc.* **1971**, *93*, 4081.

(9) Hammar, P. R.; Stone, M. B.; Reich, D. H.; Broholm, C.; Gibson, P. J.; Turnbull, M. M.; Landee, C. P.; Oshikawa, M. *Phys. Rev. B* **1999**, *59*, 1008.

(10) Mennenga, G.; de Jongh, L. J.; Huiskamp, W. J.; Reedick, J. *J. Magn. Magn. Mater.* **1984**, *44*, 89−98.

(11) Koyama, M.; Suzuki, H.; Watanabe, T. *J. Phys. Soc. Jpn.* **1976**, *40*, 1564−1569.

10.1021/cm001412+ CCC: $20.00
Published on Web 05/11/2001

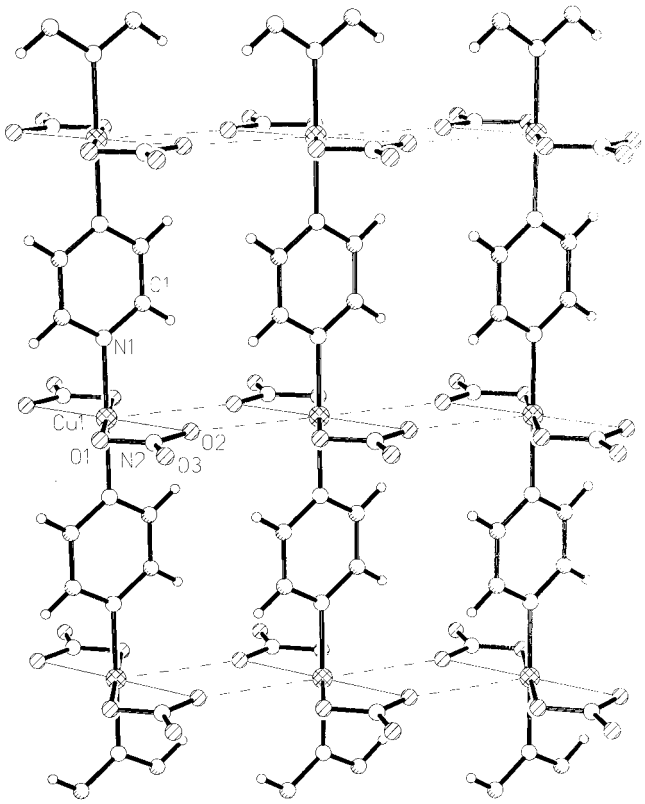

Figure 1. Crystal structure of copper pyrazine dinitrate.

one or more carbon atoms of the pyrazine ring, replacing the $S = {}^1/_2$ Cu spin sites with diamagnetic Zn atoms or isotopic substitution. In most cases the resulting magnetic properties are different from the pure compound. The strength of the superexchange interaction has recently been shown[19] to depend on the symmetry of the copper coordination sphere, which is lowered by certain methyl substitution on the pyrazine ring; the lowered symmetry induces a change in the exchange strength. Replacing Cu^{2+} ions with Zn^{2+} ions breaks the linear magnetic chain. Impurity substitution is also of interest in other transition metal oxides.[20−30]

Susceptibility measurements show that CuPzN is well described by the 1-D QHAF model, where the data are fit by the Bonner Fischer model.[9,31] The exchange constant derived from these fits is $2J/k_B = -10.4(1)$ K, which corresponds to a $T = 0$ saturation field of 14.6 T as determined by the molecular field result for $S = {}^1/_2$: $g\mu_\beta H_{sat} = 2zk_BJ$. This material is an excellent candidate for spin dynamics studies in high magnetic fields because the magnetization saturates at a field that can be attained experimentally. The saturation fields of the chemically modified materials are lower yet: Cu(mepz)-(NO_3) = 13.7(2) T, Cu(2,3-dimepz)(NO_3) = 11.3(4) T. Such tunability of magnetic properties based on the nature of the nonmagnetic bridging group allows the study of many interesting high-field properties, including random exchange effects in samples with mixed substituted pyrazines.[9,32]

While the magnetic properties of CuPzN have been studied as a function of chemical substitution, there are still unanswered questions regarding how these chemical modifications alter the elastic properties of the lattice. We have investigated the vibrational response of CuPzN and its derivatives via infrared spectroscopy to better understand the nature of the magneto-structural correlations.

II. Experimental Section

Needlelike crystals of CuPzN were grown by slow evaporation of aqueous Cu(II) nitrate and pyrazine in a 1:1 ratio.[9] Likewise, deuterated(Cu(II) NO_3 + deuterated pyrazine), Zn-doped (Cu(II)NO_3 + Zn(II)NO_3 + pyrazine), and substituted dimethylpyrazine (Cu(II)NO_3 + (2,6)dimethylpyrazine) compounds were grown by similar techniques. The pure crystals as well as the Zn-doped and deuterated samples were purple, thin needles, whereas the substituted material was darker, thicker, and longer. Zn impurity concentration was assessed by inductively coupled plasma/atomic emission spectroscopy.[33]

Polarized middle infrared (MIR) transmission spectra were taken with a Bruker Equinox 55 FTIR equipped with an IR Scope II infrared microscope. A liquid-nitrogen-cooled MCT detector was employed. Temperature control was provided by an Oxford Microstat He cryostat. Polarized 300 K far-infrared (FIR) spectra were collected at the National Synchrotron Light Source at Brookhaven National Laboratory. Data were taken on a Bruker 113V FTIR equipped with a bolometer detector at Beamline U12IR of the VUV ring.[34] Standard polarizers, filters, and beam splitters were used to cover the respective frequency ranges.

Even with the thinnest crystals, a number of vibrational bands in the aforementioned polarized spectra were saturated. To circumvent this problem, several crystals were ground with KCl (MIR) and paraffin (FIR) and pressed into pellets for unpolarized infrared measurements. The advantage of this

(12) Santoro, A.; Mighell, A. D.; Reimann, C. W. *Acta Crystallogr.* **1970**, *B26*, 979−984.
(13) Inoue, M. *J. Magn. Reson.* **1970**, *27*, 159−167.
(14) Richardson, H. W.; Hatfield, W. E. *J. Am. Chem. Soc.* **1976**, *98*, 835−839.
(15) McGregor, K. T.; Soos, Z. G. *J. Chem. Phys.* **1976**, *64*, 2506−2517.
(16) Losee, D. B.; Richardson, H. W.; Hatfield, W. E. *J. Chem. Phys.* **1973**, *59*, 3600−3603.
(17) Kokoszka, G. F.; Reimann, C. W. *J. Inorg. Nucl. Chem.* **1970**, *32*, 3229−3331.
(18) Hoffman, S. K.; Goher, M. A. S.; Hilczer, W.; Goslar, J.; Hafez, A. K. *Acta Phys. Polym.* **1994**, *85*, 517−530.
(19) Landee, C. P.; Jensen, W. E.; Woodward, F. M.; LaPierre, M. A.; Turnbull, M. M., unpublished data.
(20) Dhalenne, G.; Rouchard, J. C.; Revcolevschi, A.; Federoff, M. *Physica C* **1997**, *282−287*, 953−954.
(21) Itoh, M.; Tanaka, R.; Yamauchi, T.; Ueda, Y. *Physica B* **2000**, *281−282*, 671−672.
(22) Grenier, B.; Renard, J.-P.; Veillet, P.; Regnault, L.-P.; Lorenzo, J. E.; Paulsen, C.; Dhalenne, G.; Revcolevschi, A. *Physica B* **1999**, *259−261*, 954−955.
(23) Saint-Paul, M.; Voiron, J.; Paulsen, C.; Monceau, P.; Dhalenne, G.; Revcolevschi, A. *J. Phys. Condens. Matter* **1998**, *10*, 10215−10221.
(24) Fabrizio, M.; Mélin, R.; Souletie, J. *Eur. Phys. J. B* **1999**, *10*, 607−621.
(25) Jones, B. R.; Sushkov, A. B.; Musfeldt, J. L.; Wang, Y. J.; Revcolevschi, A.; Dhalenne, G. *Phys. Rev. B* **2001**, *63*, 134414.
(26) Coad, S.; Lussier, J.-G.; McMorrow, D. F.; McK Paul, D. *J. Phys. Condens. Matter* **1996**, *8*, 6251−6266.
(27) Maury, F.; Nicolas-Francillon, M.; Bourée, F.; Ollitrault-Fichet, R.; Nanot, M. *Physica C* **2000**, *333*, 121−132.
(28) Alff, L.; Kleefisch, S.; Meyer, S.; Schoop, U.; Marx, A.; Sato, H.; Naito, M.; Gross, R. *Physica B* **2000**, *284−288*, 591−592.
(29) Tsuei, C. C.; Kirtley, J. R. *Phys. Rev. Lett.* **2000**, *85*, 182−185.
(30) Sidis, Y.; Bourges, P.; Fong, H. F.; Keimer, B.; Regnault, L. P.; Bossy, J.; Ivanov, A.; Hennion, B.; Gautier-Picard, P.; Collin, G.; Millius, D. L.; Aksay, I. A. *Phys. Rev. Lett.* **2000**, *84*, 5900−5903.
(31) Bonner, J. C.; Fisher, M. E. *Phys. Rev.* **1964**, *135*, A640.
(32) Landee, C. P.; Turnbull, M. M. *Mol. Cryst. Liq. Cryst.* **1999**, *335*, 905−912.
(33) United States Environmental Protection Agency, SW-846, Method 6010B.
(34) Because of the extremely small size of the samples, the aperture needed for far-infrared single-crystal transmittance measurements was 100 μm. To obtain a sufficient signal to the detector in such a configuration, an intense source, like that of the synchrotron facility at Brookhaven National Laboratory, is required.

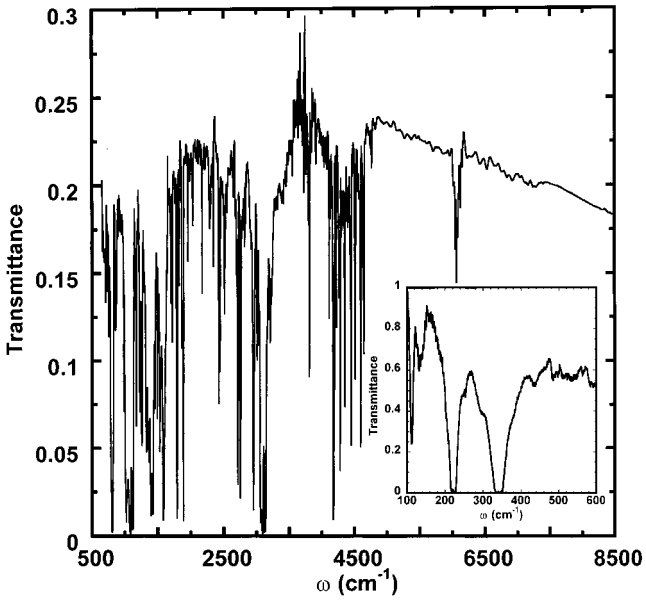

Figure 2. Single-crystal infrared transmittance spectrum of copper pyrazine dinitrate at 10 K, with light polarized parallel to the chain axis. The inset displays the far-infrared transmittance data at 300 K.

technique is that we can adjust the sample concentration to highlight a feature of interest; however, in such measurements, polarization information is lost. Temperature-dependent far-infrared and mid-infrared data were obtained using a Bruker 113V FTIR with bolometer and DTGS detectors, respectively. The pellets for the middle infrared analysis were made with KCl rather than KBr to avoid possible reduction of Cu^{2+} to Cu^{1+}.

Standard PEAKFIT procedures were used to fit the frequency-dependent absorption data. Here, absorption was estimated from the measured transmission as $\alpha(\omega) = -\ln(T(\omega))$. The raw data were fit primarily with Lorenztian peak shapes using reasonable background choices. Errors were estimated statistically, based upon 95% confidence limits of the fit parameters.

III. Results

Figure 2 shows the infrared transmittance spectrum of a single crystal of pure CuPzN with light polarized parallel to the magnetic chain direction.[35] The spectrum is very rich with a large number of intramolecular vibrations; if we consider both $\|a$ and $\perp a$ polarizations, there are more than 100 modes, attesting to the excellent wave propagating properties and insulating nature of this material. Even when extremely thin samples ($\approx 1.1 \times 0.075 \times 0.012$ mm) are used for the measurements, the absorptions are so intense that peak saturation in the transmittance spectrum cannot be avoided. Yet another peculiarity is the energies at which these features appear. The modes appear to be divided into clusters, perhaps relating to their respective order, and the structures continue up to 6000 cm^{-1}, which is very unusual.[36,37] The far-infrared regime was also explored on pure CuPzN single crystals to gain information on the first-order fundamental modes and also to help make assignments on the higher order combination and overtone modes. The majority of the peaks in the far-infrared are also saturated, but the polarization assignments are clear. Mode assignments were performed with the aid of known functional group frequencies and vibrational analyses of similar systems.[38−46]

Both paraffin and KCl isotropic pellet spectra (not shown) display fewer features overall, as we are averaging over both polarizations and many modes are superimposed. These experiments were performed to gain more control over the CuPzN concentration in the incident beam. This allows us to identify the exact resonance position of modes that were previously saturated in the single-crystal data and to track these peak positions and other mode characteristics with temperature.

Temperature-dependent measurements were performed on both single-crystal and pressed pellet samples of CuPzN in the range of 5−300 K. The most striking result is the trend of peak center vs temperature of a large number of peaks. Many of the features shift to lower frequency with decreasing temperature, and this mode "softening" occurs gradually throughout the entire temperature range of investigation. In the single-crystal data, nearly one-third of the modes soften. This trend is in contrast to the general expectation of mode hardening.[47] Figure 3 compares the temperature dependence of some representative red-shifted modes to that of the more standard blue-shifted modes. As will be shown later, this unusual softening behavior observed in CuPzN is a result of interchain hydrogen bonding.

The peak centers of features in the pure CuPzN spectra were plotted against temperature for many modes, both hardening and softening, and a representative selection is shown in Figure 4. The trends of peak area and FWHM of these vibrational modes (not shown) were also monitored, and each behaves the same way, independent of the direction of the frequency shift with temperature. There is no abrupt discontinuity in any of the trends which would indicate a phase transition in this temperature range, in agreement with previous structural, susceptibility, and specific heat data.[9,11] It

(35) The middle infrared spectrum of the single-crystal CuPzN was taken with an infrared microscope because of the small size of the samples.

(36) Transmittance measurements of C_{60} reveal a similarly rich spectrum, with higher energy modes clustered above 1500 cm^{-1}, yet features do not appear at such high energy as in CuPzN.[60]

(37) Vibrational transitions near 6000 cm^{-1} appear to be fourth-order, with the lower energy transitions being third-, second-, and first-order, respectively.

(38) *Vibrational Spectra of Polyatomic Molecules*; Swerdlov, L. M., Kovner, M. A., Krainov, E. P., Eds.; John Wiley and Sons: New York, 1974.

(39) *Infrared Characteristic Group Frequencies*; Socrates, G., Ed.; John Wiley and Sons: New York, 1980.

(40) *The Sigma Library of FT-IR Spectra, 1st ed., Vol. 2*; Keller, R. J., Ed.; Sigma Chemical Co.: St. Louis, 1986.

(41) *Infrared and Raman Spectra of Inorganic and Coordination Compounds*, 3rd ed.; John Wiley and Sons: New York, 1978.

(42) *CRC Handbook of Chemistry and Physics*, 62nd ed.; Weast, R. C., Ed.; CRC Press: Boca Raton, 1981.

(43) *Characteristic Frequencies of Chemical Groups in the Infrared*; Flett, M. C., Ed.; Elsevier: New York, 1963.

(44) Billes, F.; Mikosch, H.; Holly, S. *Theor. Chem.* **1998**, *423*, 225−234.

(45) Biagetti, R.; Bottjer, W. G.; Haendler, H. M. *Inorg. Chem.* **1966**, *5*, 379−382.

(46) Castro, P. M.; Jagodzinski, P. W. *J. Phys. Chem.* **1992**, *96*, 5296−5302.

(47) This expected behavior of vibrational modes is governed by the approximation $\omega \approx (k/\mu)^{1/2}$, where k is the spring constant characteristic of the bond and μ is the effective mass of the atoms involved in the vibration. As temperature is lowered, the unit cell is expected to contract, thereby increasing the value of k. This results in the increase of ω with decreasing temperature.

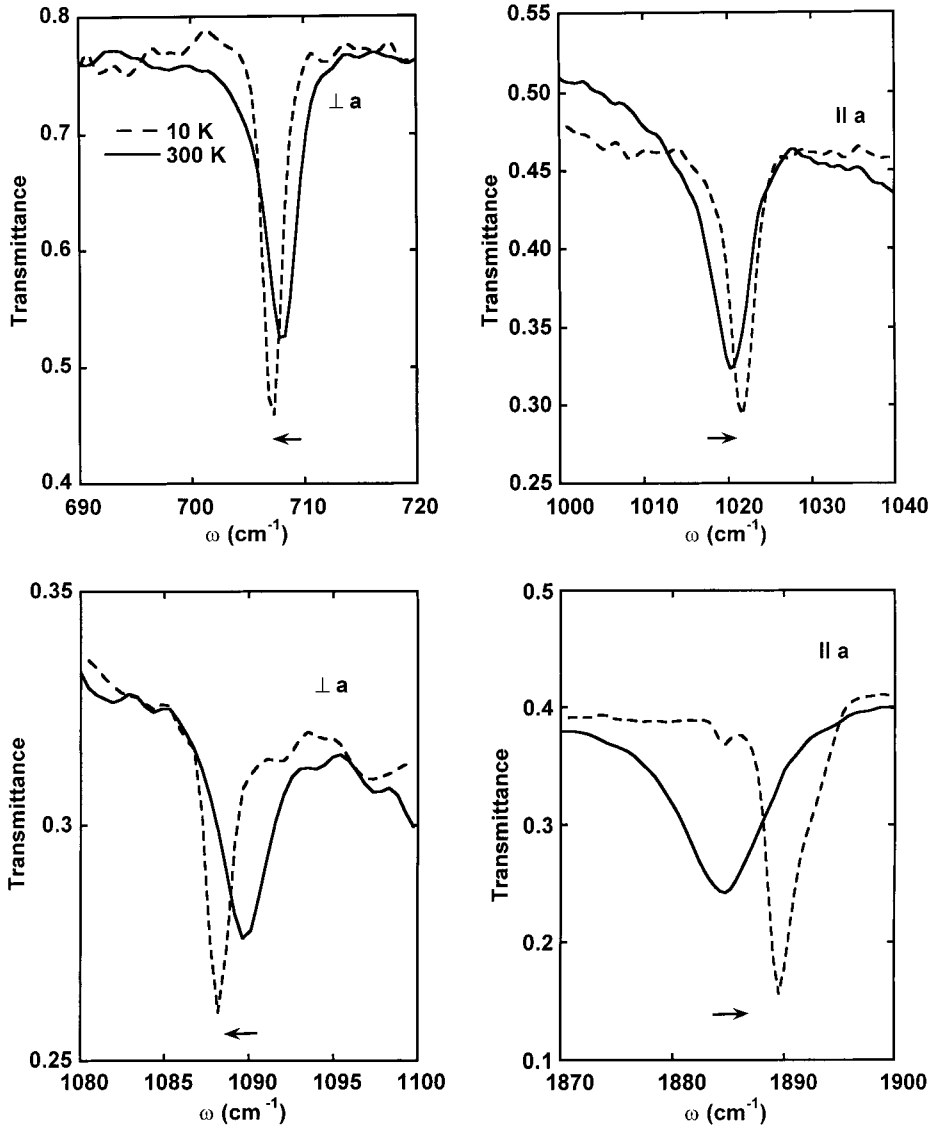

Figure 3. Representative plots of the temperature dependence of both hardening and softening modes in middle-infrared spectra of single-crystal CuPzN. The solid lines represent the spectrum at 300 K, whereas the dashed lines represent the spectrum at 10 K. The features in the left column soften with temperature (upper panel: NO_2 nonplanar deformation; lower panel: C−H out-of-plane deformation or ring stretch), and those in the right column harden (upper panel: in-plane bending of pyrazine ring; lower panel: combination or overtone). The arrows show the direction of the frequency shift, from 300 to 10 K, for clarity.

is interesting that the temperature dependence of the peak center of the modes that soften is nearly linear, whereas the trend of the modes that harden is clearly nonlinear. This distinction holds for most of the modes analyzed and seems to suggest a different physical origin for the two behaviors. The assignments of all softening modes observed in a single crystal of copper pyrazine dinitrate are shown in Table 1.

Temperature-dependent KCl pellet transmission measurements were also performed on a number of chemically modified derivatives of CuPzN, including deuterated, 2,6-dimethyl-substituted and 0.50% Zn-doped samples. The softening is less pronounced in the deuterated material and least prominent in the 2,6-dimethyl copper pyrazine dinitrate. Overall, the spectrum of Zn-doped CuPzN is quite similar to that of the pure material in the region 650−7500 cm^{-1}, and the temperature-dependent frequency shifts of all modes matched as well. Finally, the middle infrared response was measured on a KBr pellet sample of pure pyrazine as a function of temperature to ensure that the vibrational modes of pyrazine do not soften. All of the features observed in this spectrum hardened, as expected.

IV. Discussion

A. Models of Vibrational Temperature Dependence. The softened modes observed in this system are many, red-shifting over the entire temperature region (300−5 K), and generally display a small absolute frequency shift (5 cm^{-1} or less). These characteristics run counter to the standard picture of a "soft mode" as a precursor to superconductivity or a magnetic ordering temperature. That there are no structural nor magnetic transitions in this temperature range makes it necessary to investigate models of vibrational softening to discover the fundamental mechanism behind this phenomenon.

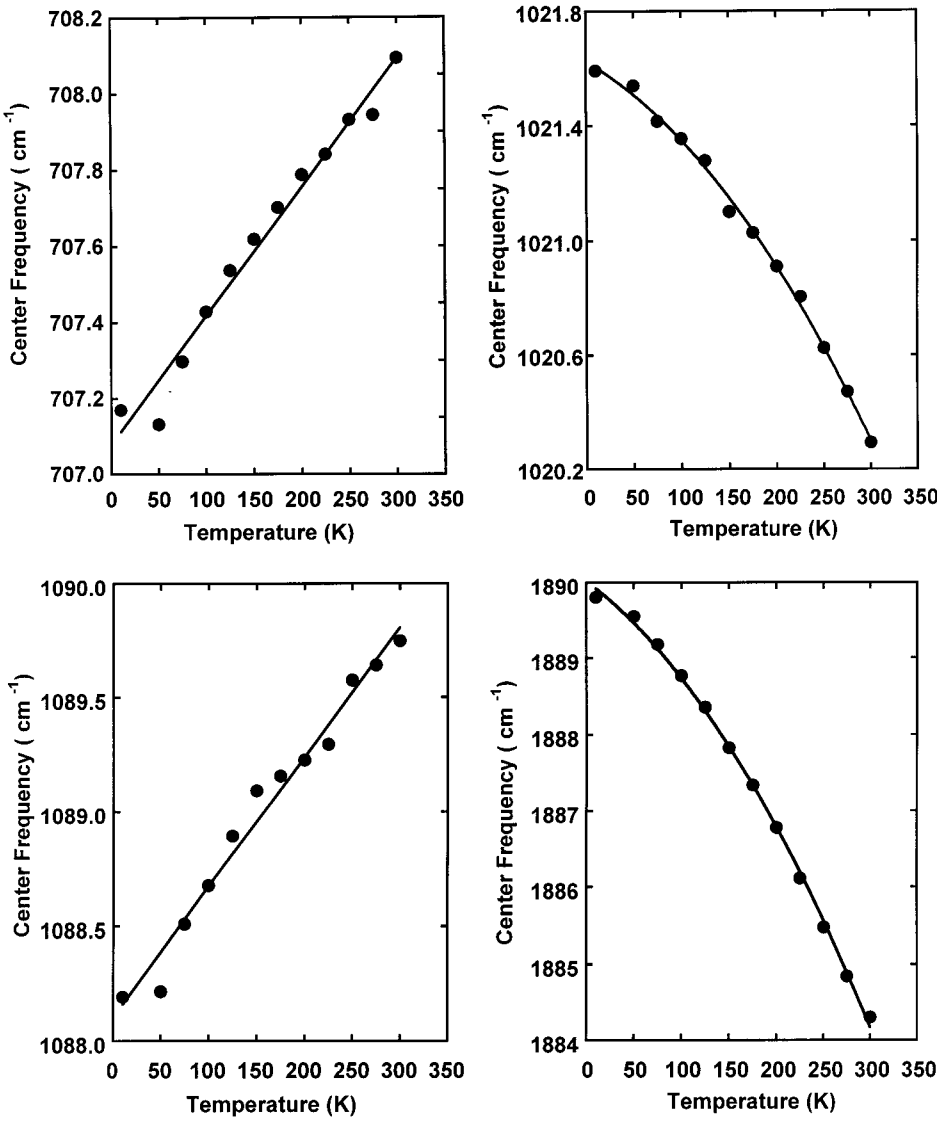

Figure 4. Trends of peak center of representative modes (the same modes as in Figure 3) vs temperature. Note the near-linearity of the trend of softening modes (left column) and nonlinearity of hardening modes (right column).

The temperature-dependent frequency change of a phonon α in magnetic materials can be written as:[48−52]

$$\omega_\alpha(T) - \omega_\alpha(T_0) \equiv \Delta\omega_\alpha(T) = (\Delta\omega_\alpha)_{\text{latt}} + (\Delta\omega_\alpha)_{\text{anh}} + (\Delta\omega_\alpha)_{\text{ren}} + (\Delta\omega_\alpha)_{\text{s-ph}} \quad (1)$$

The first term is the lattice contribution and is concerned with the change in bond strengths and lengths as the unit cell contracts/expands with temperature. It is commonly approximated by the Grüneisen law and assumes either a cubic crystal or an isotropically expanding/contracting lattice.[48,51,52] We will discuss whether this term is responsible for the softening modes in copper pyrazine dinitrate in more detail later.

The $(\Delta\omega_\alpha)_{\text{anh}}$ term accounts for the intrinsic anharmonic contribution or the anharmonicity at constant volume.[48] In CuPzN, the standard peak shapes of the softened modes remain at all temperatures and suggest that the reason for such behavior is not purely anharmonic. Further, if the modes were softening because of intrinsic anharmonicity, only higher order excitations should show this behavior. Softened modes are found throughout the spectrum (even as low as ≈700 cm^{-1}), and many are first-order.

The third term in eq 1 is the renormalization contribution. This term accounts for the renormalization of electronic states that may occur through a three-dimensional magnetic ordering temperature.[48,50] CuPzN does not order at any temperature investigated here, and on the basis of the insulating character of this material at all temperatures, this term cannot be responsible for the softening observed *throughout* the temperature region studied.

Finally, $(\Delta\omega_\alpha)_{\text{s-ph}}$ is the contribution to the change in the phonon frequency from spin−phonon interactions. The spin−phonon contribution is caused by the modulation of the exchange integral by lattice vibrations. This

(48) Granado, E.; Garcia, A.; Sanjurjo, J. A.; Rettori, C.; Torriani, I.; Prado, F.; Sánchez, R. D.; Caniero, A.; Oseroff, S. B. *Phys. Rev. B* **1999**, *60*, 11879−11882.
(49) Baltensperger, W.; Helman, J. S. *Helv. Phys. Acta* **1968**, *41*.
(50) Kim, K. H.; Gu, J. Y.; Choi, H. S.; Park, G. W.; Noh, T. W. *Phys. Rev. Lett.* **1996**, *77*, 1877.
(51) *Proceedings of the International School of Physics 'Enrico Fermi': Semiconductors*; Smith, R. A., Ed.; Academic Press: New York, 1963; pp 505−514.
(52) Kleinman, D. A. *Phys. Rev.* **1960**, *118*, 118.

Table 1. Assignments of Softening Modes in Pure Copper Pyrazine Dinitrate

position at 300 K (cm^{-1})	position at 5 K (cm^{-1})	intensity[a]	characterization
Polarized Parallel to Chain Direction			
1427.9	1426.1	s	C−H in plane bending
1494.4	1493.9	w	C−H in plane bending
1584.0	1583.6	s	N−C−H vibration of pyrazine
2348.9	2346.3	w	combination and overtone
2430.0	2426.9	m	combination and overtone
2450.0	2446.4	w	combination and overtone
2717.9	2715.3	m	combination and overtone
2766.0	2761.8	m	combination and overtone
2849.9	2846.0	m	combination and overtone
≈2920	2919.3	w	combination and overtone
3794.6	3791.9	m	combination and overtone
4195.1	4193.5	m	combination and overtone
4283.2	4281.9	s	combination and overtone
4354.2	4352.2	s	combination and overtone
4452.1	4451.5	s	combination and overtone
4597.1	4596.7	s	combination and overtone
Polarized Perpendicular to Chain Direction			
708.0	707.1	s	NO_2 nonplanar deformation
1089.7	1088.2	m	C−H out of plane deform. or ring stretch
1103.7	1101.7	w	ring stretch
2180.4	2176.0	m	combination and overtone
2491.4	2489.0	s	combination and overtone
2759.4	2757.8	s	combination and overtone
2952.4	2948.2	s	C−H stretch
3013.3	3011.0	w	C−H stretch
3100.0	3098.4	m	C−H stretch
3954.3	3950.7	w	combination and overtone
4469.6	4468.1	m	combination and overtone
4523.0	4521.3	s	combination and overtone
5929.3	5927.3	w	combination and overtone

[a] s = strong, m = medium, w = weak.

interaction was considered as a contribution to the change in a phonon frequency in europium oxide by Baltensperger and Helman[49] and was applied to a softening mode in $LaMnO_3$ by Granado et al.,[48] although in this case, the ≈610-cm^{-1} mode only began to soften below the ≈140 K magnetic ordering temperature. Because the mode softening in CuPzN takes place between 300 and 5 K and is not enhanced at an ordering temperature, this term is likely not responsible for the softening behavior. Further, estimates of the size of $(\Delta\omega_\alpha)_{s-ph}$ indicate that it is very small and unlikely to contribute here.[49]

On the other hand, a model used to describe the large Seebeck coefficients displayed in the boron carbides ($B_{12+x}C_{3-x}$) is that of carrier-induced vibrational softening. Localized carriers are known to soften the vibrations to which they are coupled because of the nonlinear dependence of their electronic energy on atomic displacements. Here, in response to an asymmetric intramolecular vibration in the crystal, there is a redistribution of the charge of a localized carrier as the atoms move. Thus, the degree of softening depends on the transfer energy of the intramolecular electronic motion.[53−55] Copper pyrazine dinitrate, however, is an insulator.[56] The absence of underlying electronic structures at lower energy and the shape of the features show the purely vibrational character of the modes and the insulating nature of this material. Therefore, we conclude that carrier-induced vibrational softening is not a suitable model for this system.

Low-temperature softening of six Raman active modes in the organic molecular building block material BEDT-TTF (neutral and d_8-BEDT-TTF) has been observed by Lin et al.[57] The authors report that the observed softening indicates a structural instability in the material (in the absence of a structural phase change) and a subsequent increase in C−H bending at low temperature, which is supported by X-ray data. This scenario has many similarities to the phenomenon observed in copper pyrazine dinitrate.

B. Spectra and Bond Length Analysis. The lattice term in eq 1 considers the change in frequency of phonons with temperature based on volume effects.[48] Because the Grüneisen approximation assumes an isotropically expanding/contracting lattice, phonons are normally expected (with regard to this term) to shift to higher energy with decreasing temperature, as the spring constants of all vibrations tighten at low temperature. The high- and low-temperature lattice parameters derived from both X-ray diffraction and neutron experiments show, however, that copper pyrazine dinitrate does not contract isotropically; the chain axis, being quite rigid, contracts less than the other two crystallographic directions.[9,12,58] Because the lattice contribution cannot be so easily explained by a simple volume approximation, it is necessary to investigate the detailed structural changes and interactions of CuPzN as temperature is lowered.

Vibrational mode softening in CuPzN interpreted within a lattice contribution picture is consistent with an increase in bond lengths related to the affected functional group signatures with reduced temperature. Table 2 compares the lengths of selected bonds in this material at both 300 and 158 K.[9,12,58] Some bond lengths are reduced with decreasing temperature, consistent with the observed mode hardening, yet others remain constant or even increase. For instance, the C−C bonds of the pyrazine moiety remain relatively constant, whereas the bonds between the nitrogen and carbon atoms of the ring increase in length with decreasing temperature. The N(2)−O(1) and N(2)−O(3) bonds also increase significantly. The C−H stretching modes observed in the spectra around 3000 cm^{-1} also tend to soften, suggesting that these bonds increase in length as well. Figure 5 displays asymmetric sections of two neighboring chains of CuPzN and specifies a number to designate each atom in the asymmetric unit for clarity.

To explain why the aforementioned bond lengths increase with decreasing temperature in the absence of negative thermal expansion coefficients, it is necessary to consider possible interactions between chains. For bonds to soften in a lattice where all three crystallographic directions contract, albeit at different rates,

(53) Emin, D. *Phys. Rev. B* **2000**, *61*, 6069−6085.
(54) Emin, D. *Phys. Rev. B* **1993**, *48*, 13691−13702.
(55) Emin, D. *Phys. Rev. B* **1999**, *59*, 6205−6210.
(56) The edge of the optical gap does not begin until ≈10 000 cm^{-1}, which is quite far away from the energy range of molecular vibrations, and no appreciable electron−phonon coupling is expected or observed.
(57) Lin, Y.; Eldridge, J. E.; Williams, J. M.; Kini, A. M.; Wang, H. H. *Spectrochim. Acta Part A* **1999**, *55*, 839−843.
(58) 300 K X-ray data taken from Santoro et al. were confirmed and found to agree within the standard deviation values reported. The crystal structure data have been deposited with the CCDC, reference #158874.

Table 2. Comparison of Selected Bond Lengths and Angles of Pure Copper Pyrazine Dinitrate at 300 and 158 K

	distance[a] at 300 K (Å)	distance[b] at 158 K (Å)		angle[a] at 300 K (deg)	angle[b] at 158 K (deg)
			Coordination Sphere		
Cu−N(1)	1.984(4)	1.974(3)	N(1)−Cu−O(1 or 2)	90	90
Cu−O(1)	2.010(4)	2.004(3)	O(1)−Cu−O(2)	56.11(17)	56.88(9)
Cu−O(2)	2.490(5)	2.478(3)			
			Nitrate Group		
N(2)−O(1)	1.287(7)	1.295(4)	O(1)−N(2)−O(2)	116.71(48)	117.6(3)
N(2)−O(2)	1.249(7)	1.247(4)	O(1)−N(2)−O(3)	119.30(50)	118.7(3)
N(2)−O(3)	1.214(7)	1.227(4)	O(2)−N(2)−O(3)	123.99(55)	123.7(3)
			Pyrazine Molecule		
N(1)−C(1)	1.330(5)	1.339(3)	C(1)−N(1)−C(1)	118.73(36)	118.8(3)
C(1)−C(1′)	1.387(5)	1.387(4)	N(1)−C(1)−C(1′)	120.64(37)	120.61(15)
C(1)−H(1)	0.93(7)				

[a] 300 K data were taken from Santoro et al.[12,58] [b] 158 K data were taken from Hammar et al. and unpublished data.[9,58]

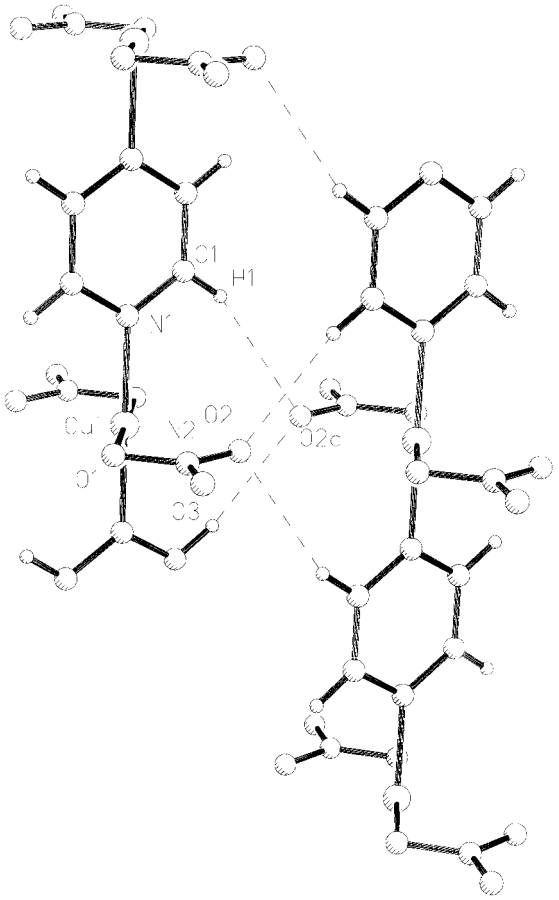

Figure 5. A section of two neighboring chains of copper pyrazine dinitrate, highlighting both the number designation of the atoms in the asymmetric unit and the proposed interchain electrostatic interaction.

there must be competing interactions. Because of the arrangement of the nitrate ions and the pyrazine molecule, an electrostatic attraction between the pyrazine hydrogens and the oxygens of the nitrates is possible. The distance between C(1) and O(2) within each chain, however, is much greater than 3 Å, making this intrachain interaction unlikely. The distance between the carbon of the pyrazine and the oxygen of a nitrate ion on a *neighboring* chain turns out to be 3.459 Å at 300 K.[58] This distance becomes smaller as the temperature is lowered (3.443 Å at 158 K), making the interchain hydrogen bond more favorable. Because of the anisotropic thermal expansion of the crystal caused by the rigidity of the chain axis (*a*), this electrostatic interaction strengthens more rapidly than the overall lattice contraction. This attraction may pull the hydrogen and the oxygen together, causing increased C−H and N(1)−C(1) bond lengths and a spreading of the nitrate ion. The hydrogen bond competes with the lattice contraction along *a*, leaving the C−C′ bond distance unchanged with decreasing temperature. This is because the neighboring hydrogen bond interaction of the same ring produces an attraction on C′ with a component in the *a* direction opposite to that on C. The weak hydrogen bonding between chains is highlighted in Figure 5 with a dashed line.

Table 3. Frequency Shift of NO_2 Nonplanar Deformation Mode in Pure, Deuterated, and 2,6-Dimethyl-Substituted Copper Pyrazine Dinitrate in KCl

material	ω (cm^{-1}) at 300 K	ω (cm^{-1}) at 5 K	$\Delta\omega$ (cm^{-1})
pure CuPzN	707.72	706.83	0.89
2,6-dimethyl CuPzN	707.12	706.50	0.62
deuterated CuPzN	707.68	706.98	0.70

C. Chemical Substitution Effects. An attractive property of the CuPzN system is the ability to alter the structure in a variety of ways. There are a number of methods with which to modify the pyrazine ring alone; methyl groups can be placed on the ring in different configurations and the hydrogen atoms may be replaced by deuterium.[9] This tunability can be used as a tool to test the hydrogen-bonding interaction hypothesis as the origin of the vibrational softening.

Substituting methyl groups to the pyrazine ring of CuPzN significantly interferes with the interchain electrostatic interaction, both because two hydrogen atoms have been replaced by CH_3 and steric effects should drive the remaining hydrogens further away from the oxygen atoms. When hydrogen atoms of the pyrazine ring are replaced by deuterium, the electrostatic attraction is expected to be similar to the pure compound (while deuterium is heavier, the electronegativity is unchanged). Because of the difference in mass, however, we anticipate that the C−D bond length will not increase as quickly with decreasing temperature and that the overall softening observed in the vibrational modes of (D_4)CuPzN should therefore be less pronounced.

We have measured both 2,6-dimethyl and deuterated copper pyrazine dinitrate as a function of temperature to test these predictions. Table 3 compares the magnitude of the softening observed in pure, deuterated, and 2,6-dimethyl-substituted copper pyrazine dinitrate. Here,

the frequency shift of a NO_2 nonplanar deformation mode is used as a measure of the degree of overall softening in each material. As expected, the change in frequency of this mode is the greatest for pure CuPzN, less for the deuterated material, and least for the 2,6-dimethyl-substituted compound. CuPzN doped with 0.50% Zn was also measured, but no difference in $\Delta\omega$ was noticed from that observed in the pure material. Because doping with Zn does not interfere with the electrostatic interaction of the hydrogens of the pyrazine and the oxygens of the nitrate ion, this result is also expected.

Recent studies[19,59] of the crystal structures of the methyl-substituted Cu(sub-pz)$(NO_3)_2$ chains have provided insight into the variation of exchange strengths within this family of compounds. Structures are now known for Cu(2-mepz)$(NO_3)_2$, Cu(2,3-dmpz)$(NO_3)_2$, and Cu(2,5-dmpz)$(NO_3)_2$ for which the antiferromagnetic exchange strengths are 9.5, 8.1, and 10.2 K, respectively. The crystal structure of Cu(2,6-dmpz)$(NO_3)_2$ ($J/k = 10.9$ K) has not yet been determined.

The effects of methyl substitution are 2-fold. The decreased symmetry of the substituted pyrazine molecule lowers the symmetry of the copper sites in the Cu(2-mepz)$(NO_3)_2$and Cu(2,3-dmpz)$(NO_3)_2$ chains, such that the copper atom sits above the local basal plane and the trans N−Cu−N and O−Cu−O angles are less than 180°. Such changes decrease the orbital overlap of the copper $d_{x^2-y^2}$ orbital onto the pyrazine ring and can account for the reduction in exchange strengths for these two compounds.

The additional steric bulk of the substituted pyrazine molecules also affects the patterns in which the chains are packed into three-dimensional lattices but without significantly altering the hydrogen-bonding patterns. In CuPzN, hydrogen bonding between the ring hydrogens and nitrate O(2) atoms of adjacent chains is found with a C−O(2) distance of 3.443 Å at 158 K. In both the mepz and 2,3-dmpz analogues, the chains along the *a* axis form layers in the *ac* planes. The methyl substituents on the pyrazine rings are oriented in double layers such that the methyl groups of adjacent sheets face each other, with the hydrogens attached to C(5) and C(6) facing each other in the alternate layers. As a result, the distance between the planes of copper atoms alternates.

On the basis of X-ray structural data, hydrogen bonding similar to that found in CuPzN is likely to occur between the ring hydrogens and O(2) atoms from adjacent planes for the methylpyrazine and 2,3-dimethylpyrazine analogues, with C−O(2) distances of 3.47 and 3.48 Å, respectively. No favorable hydrogen-bonding condition involving the methyl groups is anticipated for any of the structures. In Cu(2,5-dmpz)$(NO_3)_2$ the packing of chains is very different, consistent with the lower symmetry of the $P1$ space group. Hydrogen bonding is likely between O(2) of one chain and the hydrogen of a ring carbon on the adjacent chain. The C−O(2) bond distance (3.36 Å) is even smaller in this compound, suggesting that the interaction may even be enhanced relative to CuPzN. The structure of the 2,6-dmpz analogue is not yet known, but the softening of the vibrational modes observed here suggests that the hydrogen bonds found within it form networks similar to those observed in the other members of the copper substituted pyrazine family.

V. Conclusion

The infrared spectrum of CuPzN is characteristic of an insulator, with an extraordinary number of vibrational modes that continue to energies as high as 6000 cm^{-1}. These measurements reveal many modes in copper pyrazine dinitrate that unexpectedly soften with decreasing temperature. We propose that this softening is caused by certain bond lengths that increase with decreasing temperature due to an interchain electrostatic interaction that competes with the overall thermal contraction of the lattice. This conclusion is supported by an updated analysis of previous X-ray data. Temperature-dependent infrared measurements of chemically modified CuPzN materials also support this scenario; the degree of softening is more pronounced with the pure sample than in 2,6-dimethyl-substituted CuPzN, where hydrogen bonding is less favorable. That softening modes are observed in pure CuPzN as well as all of the chemically modified compounds investigated here suggests that interchain hydrogen bonding is important to this whole class of materials and perhaps to other linear chain molecular magnetic systems.

Acknowledgment. Funding from the Division of Materials Research at the National Science Foundation (Grant DMR-9623221) is gratefully acknowledged for work at the State University of New York at Binghamton. I.O. thanks the National Science Foundation and North Atlantic Treaty Organization for fellowship support (DGE-9804462). C.P.L. and M.M.T. acknowledge the financial support from the National Science Foundation (Grant DMR-9803813). This work has benefited from stimulating discussions with N. S. Dalal, D. Emin, and C. C. Homes. We thank D. G. Rathbun for the trace metal analysis of the zinc-doped samples.

CM001412+

(59) Amaral, S.; Jensen, W. E.; Landee, C. P.; Turnbull, M. M.; Woodward, F. M. *Polyhedron*, in press.

(60) Martin, M. C.; Du, X.; Kwon, J.; Mihaly, L. *Phys. Rev. B* **1994**, *50*, 173−183.